Spectrally Augmented Hartley Transform Precoded Asymmetrically Clipped Optical OFDM for VLC

Ali Waqar Azim, Yannis Le Guennec, Ghislaine Maury

Spectrally Augmented Hartley Transform Precoded Asymmetrically Clipped Optical OFDM for VLC

Ali W. Azim, Yannis Le Guennec, and Ghislaine Maury

***Abstract*—In this letter, we propose layered discrete Hartley transform (DHT)-spread asymmetrically clipped optical-orthogonal frequency division multiplexing (LDHTS-ACO-OFDM); which employs DHT for multiplexing/demultiplexing and pulse-amplitude modulation (PAM) alphabets. LDHTS-ACO-OFDM yields several concrete and significant improvements over classical layered asymmetrically clipped O-OFDM (LACO-OFDM), such as, low peak-to-average power ratio (PAPR), low computational complexity, 3 dB improvement in bit error rate (BER), and low optical power penalty considering multipath visible light communication (VLC) channel and bandwidth limitation of light emitting diode (LED) in combination with its driver. Besides, LDHTS-ACO-OFDM enhances the spectral efficiency of conventional DHTS-ACO-OFDM, and ousts the degrading impact on BER and optical power penalty because of higher order PAM alphabets in dispersive channel.**

***Index Terms*—Intensity modulation-direct detection, optical-orthogonal frequency division multiplexing, peak-to-average power ratio.**

I. Introduction

VISIBLE light communications (VLC) is preceived as a complementary technology to overcome the looming radio-frequency (RF) spectral crisis. Along with some compelling advantages, such as, license free unlimited optical bandwidth, high-security and no electromagnetic interference, VLC is particularly appealing as it concurrently provides lighting and communication.

For VLC, optical-orthogonal frequency division multiplexing (O-OFDM) is an effective approach, as it offers high data-rate, simple one-tap equalization in the frequency-domain (FD), and an inherent resilience to combat inter-symbol-interference (ISI) [1], [2]. In VLC, O-OFDM operates using intensity modulation-direct detection (IM-DD), for which the time-domain (TD) signal is constrained to be real-valued and non-negative. Several tailored O-OFDM schemes satisfying IM-DD constraints, such as, direct-current (DC)O-OFDM [1], asymmetrically clipped (AC)O-OFDM [2] and pulse-amplitude modulation-discrete multi-tone (PAM-DMT) [3] etc. have been proposed. ACO-OFDM and PAM-DMT are power efficient compared to DCO-OFDM for lower order modulations alphabets, howbeit, have half the spectral efficiency of DCO-OFDM. To increase the spectral efficiencies of ACO-OFDM and PAM-DMT toward that of DCO-OFDM, the so-called *hybrid* techniques, such as, layered ACO-OFDM (LACO-OFDM) [4], [5] and augmented spectral efficiency (ASE)-DMT [6], respectively, have been introduced. These schemes maintain power advantage over DCO-OFDM without relinquishing half of the spectral efficiency.

One practical limitation of O-OFDM schemes, including both LACO-OFDM and ASE-DMT is high peak-to-average-power ratio (PAPR), which exacerbates non-linear distortions from the light emitting diode (LED) [7]. Besides, limited resolution converters further circumscribe the performance [7]. Albeit, numerous approaches exist to counteract high PAPR of ACO- and DCO-OFDM, but, their candid implementation to hybrid approaches is cumbersome. Recently, Zhang *et al.* [5] introduced a PAPR reduction approach for LACO-OFDM based on tone injection, however, it is associated with a substantial complexity overhead.

Wu *et al.* [8] have identified that Hermitian symmetry (HS) prerequisite to attain real-valued TD signal contributes to an increase of PAPR. Thus, it is analyzed that DHT-spread ACO-OFDM (DHTS-ACO-OFDM) [9], which averts HS, features low PAPR. Regardless, we shall establish that DHTS-ACO-OFDM experiences an increased optical power penalty and bit error rate (BER) degradation in a dispersive channel.

In this letter, we propose layered DHTS-ACO-OFDM (LDHTS-ACO-OFDM) to augment the spectral efficiency and oust the limitations of DHTS-ACO-OFDM. To the best of our knowledge, a hybrid implementation for a precoded approach has never been investigated. LDHTS-ACO-OFDM superimposes layers of DHTS-ACO-OFDM, thus, virtually occupying all the subcarriers for simultaneous transmission. We demonstrate that LDHTS-ACO-OFDM manifests lower PAPR, experiences less optical power penalty, is less complex, and sustains a 3 dB BER gain over LACO-OFDM in a dispersive channel; which includes a multipath VLC channel and a bandwidth limited LED/LED driver combination.

II. Layered DHTS-ACO-OFDM

N-order inverse DHT (IDHT) and DHT for an arbitrary FD signal, $R(k) \in \mathbb{R}$, and an arbitrary TD signal, $r(n) \in \mathbb{R}$, respectively, is defined as $r(n) = \mathrm{IDHT}\left[R(k)\right] = N^{-1/2}\sum_{k=0}^{N-1} R(k)\mathrm{cas}\left(2\pi kn/N\right)$, and $R(k) = \mathrm{DHT}\left[r(n)\right] = N^{-1/2}\sum_{n=0}^{N-1} r(n)\mathrm{cas}\left(2\pi kn/N\right)$, with $\{n,k\} = 0,1,\cdots,N-1$, and $\mathrm{cas}(\cdot) = \cos(\cdot)+\sin(\cdot)$. The kernel for both IDHT and DHT is similar, so, conveniently, the same algorithm can perform both operations [9].

The transmitter of LDHTS-ACO-OFDM is illustrated in Fig. 1. We consider N subcarriers and L layers. For lth layer, the input bit stream is mapped onto $N/2^l$ PAM symbols, i.e., $s^{(l)}\left(n^{(l)}\right), n^{(l)} = 0,1,\cdots,N/2^l-1$. Subsequently, via $N/2^l$-order DHT, the TD symbols, $s^{(l)}\left(n^{(l)}\right)$, are DHT precoded as $S^{(l)}\left(k^{(l)}\right) = \mathrm{DHT}\left[s^{(l)}\left(n^{(l)}\right)\right],\ k^{(l)} = 0,1,\cdots,N/2^l-1$.

The authors are with Université Grenoble Alpes, CNRS, Institute of Engineering, Grenoble INP, IMEP-LAHC, F-38000 Grenoble, France (email: {azima, leguennec, ghislaine.maury}@minatec.grenoble-inp.fr).

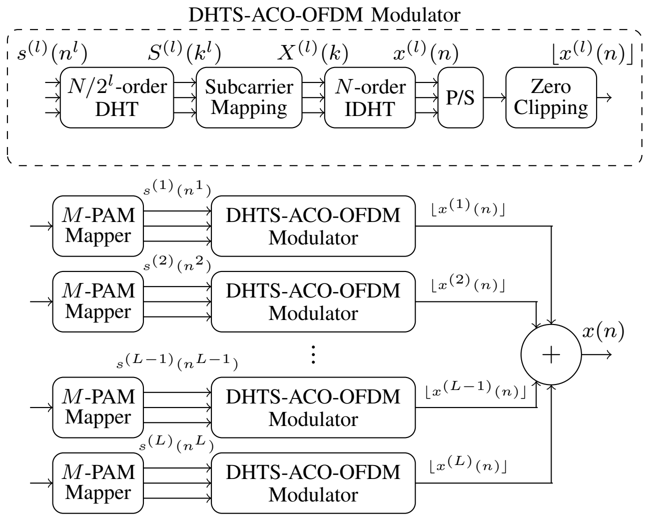

Fig. 1: Block diagram of LDHTS-ACO-OFDM transmitter.

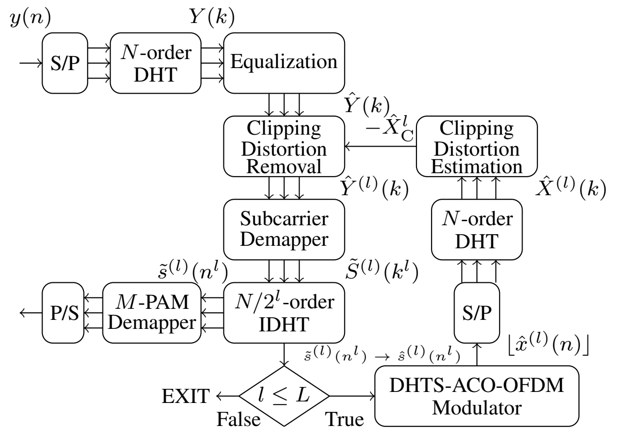

Fig. 2: Block diagram of LDHTS-ACO-OFDM receiver.

These $N/2^l$ FD DHT precoded symbols, $S^{(l)}\left(k^{(l)}\right)$, are assigned to N-length signal, $X^{(l)}(k),\ k=0,1,\cdots,N-1$, such that $X^{(l)}(k) = S^{(l)}\left(k^{(l)}\right)\ \forall\ k = 2^{l-1}\left(2k^{(l)}+1\right)$, while all the other subcarriers of the corresponding layer are set to zero. After N-order IDHT, an anti-symmetric signal, $x^{(l)}(n) = \mathrm{IDHT}\left[X^{(l)}(k)\right], n = 0,1,\cdots,N-1$ is obtained, where $x^{(l)}\left(n^{(l)}\right) = -x^{(l)}\left(n^{(l)}+N/2^l\right)$, and for $l>1$, $x^{(l)}(n) = x^{(l)}\mathrm{mod}\left(n, N/2^{l-1}\right)$, with $\mathrm{mod}(\cdot,N)$ being the modulo N operator. $x^{(l)}(n)$ is clipped at zero to yield

$$\lfloor x^{(l)}(n)\rfloor = \begin{cases} x^{(l)}(n), & x^{(l)}(n) \geq 0 \\ 0, & x^{(l)}(n) < 0 \end{cases} = x_{\mathrm{D}}^{(l)}(n) + x_{\mathrm{C}}^{(l)}(n) \quad (1)$$

for $n=0,1,\cdots,N-1$, without loss of useful information. $\lfloor\cdot\rfloor$ represents the clipping operation. $x_{\mathrm{D}}^{(l)}(n)$ and $x_{\mathrm{C}}^{(l)}(n)$ represents the lth layer data-carrying signal after clipping and the clipping distortion, respectively. The indexes $k_{\mathrm{D}}^{(l)} = 2^{l-1}\left(2k^{(l)}+1\right)$ and $k_{\mathrm{C}}^{(l)} = 2^l k^{(l)}$ identifies lth layer data-carrying subcarriers and the subcarriers affected by the clipping distortion, respectively. Subsequently, $\lfloor x^{(l)}(n)\rfloor,\ l = 1,2,\cdots,L$ are combined as

$$x(n) = \sum_{l=1}^{L} \lfloor x^{(l)}(n)\rfloor,\ n=0,1,\cdots,N-1, \quad (2)$$

which is transmitted throught the LED. In what follows, we consider perfect synchronization [7]. Since, the nonlinearity of the LED can be mitigated using digital pre-distortion [10], henceforth, we recognize a linear response of the LED.

The receiver of LDHTS-ACO-OFDM is depicted in Fig. 2. At the receiver, the light intensity is photo-detected using a photo-diode (PD). The intensity waveform is amplified using a transimpedance amplifier (TIA), and fed to an analog-to-digital converter (ADC) to yield $y(n) = h(n)\otimes x(n) + w(n),\ n=0,1,\cdots,N-1$, where $h(n)$ are the channel impulse response (CIR) coefficients, $w(n)$ represents the additive white Gaussian noise (AWGN) samples, and $\otimes$ is the convolution operator. $y(n)$ is fed to N-order DHT by which FD received signal is obtained as $Y(k) = \mathrm{DHT}[y(n)] = H(k)X(k) + W(k),\ k=0,1,\cdots,N-1$, where $H(k)$ is the channel frequency response for the kth subcarrier. After a single-tap equalization, we get

$$\hat{Y}(k) = X(k) + Z(k) = \sum_{l=1}^{L}\hat{X}_{\mathrm{D}}^{(l)} + \sum_{l=1}^{L}\hat{X}_{\mathrm{C}}^{(l)} + Z(k), \quad (3)$$

where $Z(k) = W(k)/H(k)$. $\hat{X}_{\mathrm{D}}^{(l)}$ and $\hat{X}_{\mathrm{C}}^{(l)}$ are the received FD counterparts of $x_{\mathrm{D}}^{(l)}$ and $x_{\mathrm{C}}^{(l)}$, respectively. The data on different layers is detected on a layer-to-layer basis. For layer 1, no clipping distortion falls on data-carrying subcarriers, i.e., $\hat{X}_{\mathrm{C}}^{(1)} = 0$ thus, $\hat{Y}^{(1)}(k) = \hat{Y}(k)$, from which the data-carrying subcarriers are obtained as $\tilde{S}^{(1)}\left(k^{(1)}\right) = \hat{Y}^{(1)}\left(k_{\mathrm{D}}^{(1)}\right)$. Thereafter, DHT decoding is performed via $N/2$-order IDHT, i.e., $\tilde{s}^{(1)}\left(n^{(1)}\right) = \mathrm{IDHT}[\tilde{S}^{(1)}\left(k^{(1)}\right)]$. Finally, the transmitted data on layer 1 can be detected as $\hat{s}^{(1)}\left(n^{(1)}\right) = \arg\ \min_{X\in\mathcal{S}} \|2\tilde{s}^{(1)}\left(n^{(1)}\right) - X\|,\ n^{(1)} = 0,1,\cdots,N/2-1$, where $\mathcal{S}$ denotes the constellation set of the modulation.

For layers $l>1$, the clipping distortion affecting the data-carrying subcarriers comes from $(l-1)$th layer, so, we have $\hat{Y}^{(l)}(k) = \hat{Y}^{(l-1)}(k) - \hat{X}_{\mathrm{C}}^{(l)}$. An estimate of the clipping distortion on lth layer, $\hat{X}_{\mathrm{C}}^{(l)}$ is recreated using $\lfloor\hat{x}^{(l-1)}(n)\rfloor$ which is obtained utilizing $\hat{s}^{(l-1)}\left(n^{(l-1)}\right)$. The data-carrying subcarriers for layers $l>1$ are obtained as $\tilde{S}^{(l)}\left(k^{(l)}\right) = \hat{Y}^{(l)}\left(k_{\mathrm{D}}^{(l)}\right)$ which are DHT decoded using $N/2^l$-order IDHT to have $\tilde{s}^{(l)}\left(n^{(l)}\right) = \mathrm{IDHT}[\tilde{S}^{(l)}\left(k^{(l)}\right)]$. Identical to layer 1, the transmitted symbols on layer $l>1$ can be detected as

$$\hat{s}^{(l)}\left(n^{(l)}\right) = \arg\ \min_{X\in\mathcal{S}} \left\|2\tilde{s}^{(l)}\left(n^{(l)}\right) - X\right\|, \quad (4)$$

for $n^{(l)} = 0,1,\cdots,N/2^l-1$.

Considering same modulation alphabets for all layers, we adopt fair power allocation scheme, where the electrical power appropriated to a layer correlates to the number of data-carrying subcarriers. Thus, the average electrical power of lth layer, $P_{(\mathrm{elec})}^{(l)}$, is half of $(l-1)$th layer, $P_{(\mathrm{elec})}^{(l-1)}$, yielding $P_{(\mathrm{elec})}^{(l)} = (1/2)P_{(\mathrm{elec})}^{(l-1)},\ l=2,3,\cdots,L$, with $P_{(\mathrm{elec})}^{(1)} = (M^2-1)/12$, where M is the PAM alphabet size.

Unlike most O-OFDM approaches, in which atmost half of the subcarriers are data-carrying due to HS, in LDHTS-ACO-

OFDM, since, HS is no longer required, all the subcarriers can carry data if sufficient number of layers are superimposed (theoretically $L = \infty$).

III. Performance Analysis And Discussion

Firstly, we study PAPR attributes manifested by various hybrid approaches. Further on, BER performance, and optical power penalty relative to On-Off Keying (OOK) in a dispersive channel is evaluated. Lastly, we compute the complexity exhibited by LDHTS-ACO-OFDM and LACO-OFDM. Spectral efficiency, η in bits/s/Hz for LDHTS-ACO-OFDM, LACO-OFDM, DHTS-ACO-OFDM and DCO-OFDM is expressed as $\log_2(M)[\sum_{l=1}^{L}(N/2^l)/N]$, $\log_2(\tilde{M})[\sum_{l=1}^{L}(N/2^{l+1})/N]$, $\log_2(M)[(N/2)/N]$ and $\log_2(\tilde{M})[(N/2-1)/N]$, respectively, where $\tilde{M}$ is quadrature-amplitude modulation (QAM) alphabet size. Unless otherwise mentioned, the 3 dB optical cut-off frequency of the LED with an optimized driver is set at $f_{3\text{dB}} = 150$ MHz [11], and all the results are averaged over 2000 runs with $N = 1024$. For BER and optical power penalty analysis, we consider a dispersive channel, where the dispersions are characterized by multipath VLC propagation and bandwidth limitation of LED in combination with its driver. Thus, the overall CIR is given as $h(n) = h_{\text{LED}}(n) \otimes h_{\text{chan}}(n)$, where $h_{\text{LED}}(n)$ denotes the impulse response of the LED, and $h_{\text{chan}}(n)$ are the multipath VLC channel coefficients. $h_{\text{LED}}(n)$ is modeled as a Gaussian low-pass filter having a transfer function, $H_{\text{LED}}(f) = \exp[-\ln(2)\,(f/f_{3\text{dB}})^2]$ [11]. Moreover, $h_{\text{chan}}(n)$ is obtained using recursive ray tracing algorithm for indoor VLC [12]. The transmitter and the receiver are perfectly synchronized, such that, the channel is tapped from the time of the arrival of line-of-sight (LOS) signal. A sampling time of 1 ns and up to 4 diffused reflections are considered.

A. PAPR Performance

Complementary cumulative distribution function (CCDF) curves for LDHTS-ACO-OFDM, LACO-OFDM, DHTS-ACO-OFDM, DCO-OFDM, ASE-DMT, and enhanced unipolar-OFDM (eU-OFDM) [13] for $\eta = 1$ bits/s/Hz are depicted in Fig. 3. We use $L = 5$ for LDHTS-ACO-OFDM and LACO-OFDM and 5 depths for ASE-DMT and eU-OFDM. The CCDF curves indicate that LDHTS-ACO-OFDM distinctly has the lowest PAPR, with a gain of almost 2.4 dB, 0.8 dB, 3.2 dB, 3.1 dB and 3.4 dB over LACO-OFDM, DHTS-ACO-OFDM, DCO-OFDM, ASE-DMT and eU-OFDM, respectively, at CCDF $= 0.1$. A similar progression is expected for $\eta > 1$ bits/s/Hz. The reduced PAPR results in power gain as higher modulation power can be attained after the digital-to-analog converter (DAC). Besides, cost of the converters can also be reduced.

B. Bit Error Rate Performance

The bandwidth (BW) of transmitted signal for both $\eta = \{1, 2\}$ bits/s/Hz is set at 200 MHz thus, culminating a notable impact of bandwidth limitation of the LED/LED driver combination. BER performance against electrical signal-to-noise ratio (SNR) per bit, $E_{\text{b}_{(\text{elec})}}/N_0$ for $\eta = 1$ bits/s/Hz and $\eta = 2$ bits/s/Hz is displayed in Fig. 4(a) and Fig. 4(b), respectively. We use $L = 5$ for LDHTS-ACO-OFDM and LACO-OFDM. It may be noticed that the BER of DHTS-ACO-OFDM drastically degrades from $\eta = 1$ bits/s/Hz to $\eta = 2$ bits/s/Hz because of the degrading impact of the dispersive channel on higher order modulation alphabets; which are required for $\eta = 2$ bits/s/Hz. This issue is rectified in LDHTS-ACO-OFDM; where lower order modulation alphabets can achieve higher spectral efficiences because of the superimposed structure. Moreover, the BER performance of LDHTS-ACO-OFDM is superior compared to both LACO-OFDM and DCO-OFDM. LDHTS-ACO-OFDM maintains a 3 dB gain over LACO-OFDM, because of an averaging effect of the DHT decoder which results in a same SNR for all subcarriers, whereas, for a system without precoding like LACO-OFDM, the SNR varies for each subcarrier [14].

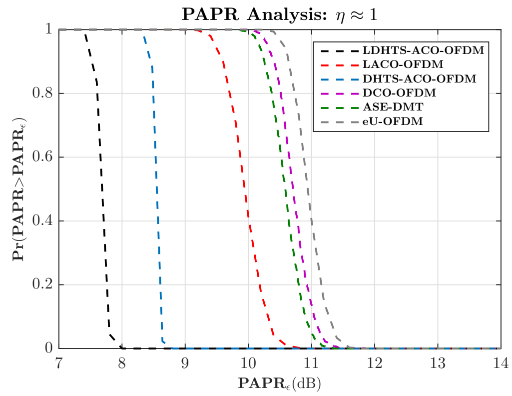

Fig. 3: CCDF curves for PAPR analysis of different modulation schemes.

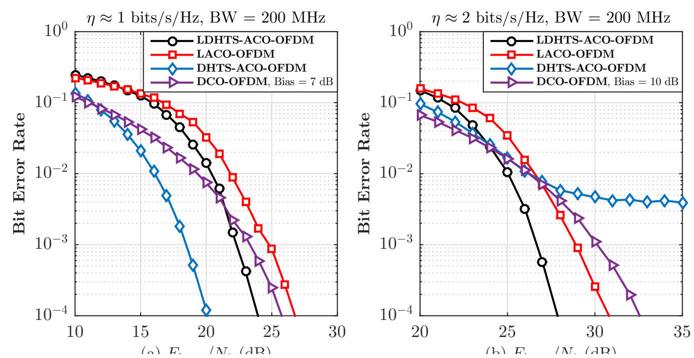

Fig. 4: BER vs $E_{\text{b}_{(\text{elec})}}/N_0$ (a) $\eta = 1$ bits/s/Hz (b) $\eta = 2$ bits/s/Hz.

C. Optical Power Penalty

For a given BER, P_b, optical power penalty is obtained by normalizing the required optical power by the average optical power needed for OOK, $E_{\text{b}_{(\text{opt})}}^{\text{OOK}}/N_0$, in an AWGN channel with no bandwidth limitation. $E_{\text{b}_{(\text{opt})}}^{\text{OOK}}/N_0$ to achieve P_b is obtained as $E_{\text{b}_{(\text{opt})}}^{\text{OOK}}/N_0 = \text{erfc}^{-2}\,(2P_\text{b})$, where $\text{erfc}(\cdot)$ is the complementary error function. Considering a dispersive channel, $P_\text{b} = 10^{-3}$, and $\eta = 2$ bits/s/Hz, the optical power penalty is obtained by varying the ratio of data-rate to the 3 dB cut-off frequency, i.e., $R_\text{b}/f_{3\text{dB}}$, as presented in Fig. 5. It is recognized that LDHTS-ACO-OFDM suffers low optical power penalty compared to LACO-OFDM for high data-rates due to precoding, whereas, for low data-rates, the optical power penalty for both LDHTS-ACO-OFDM and LACO-OFDM is essentially the same. Conventional DHTS-ACO-OFDM incurs considerably high optical power penalty because of the requirement of higher order modulation alphabets to achieve $\eta = 2$ bits/s/Hz. Moreover, DCO-OFDM experiences the largest optical power penalty because of the required bias.

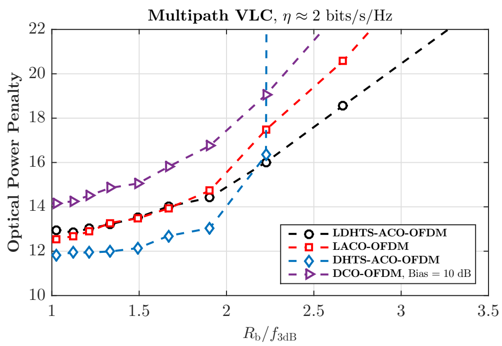

Fig. 5: Optical power penalty of different modulation schemes.

D. Complexity Analysis

The complexities of LACO-OFDM and LDHTS-ACO-OFDM are evaluated by computing the total number of required arithmetic operations at the transceiver. Discrete Fourier transform (DFT) and inverse DFT (IDFT) is implemented using fast Fourier transform (FFT) and inverse FFT (IFFT) algorithms, respectively. An N-order FFT/IFFT approximately require $4N\log_2(N)$ arithmetic operations [15], whereas, N-order DHT/IDHT nearly requires $2N\log_2(N)$ arithmetic operations [16]. Considering the complexity incurred owing to IFFT/FFT and IDHT/DHT, LACO-OFDM and LDHTS-ACO-OFDM require $\mathcal{C}^{\mathrm{LACO}} = 4N\log_2(N)[3L-1]$ and $\mathcal{C}^{\mathrm{LDHTS}} = 2N\log_2(N)[3L-1] + (N/2^{L-2})[\log_2(N) - L] + 6\sum_{l=1}^{L-1}(N/2^l)\log_2(N/2^l)$ operations, respectively. We introduce relative gain parameter, $\mathcal{G}(N,L) = \left[1 - \left(\mathcal{C}^{\mathrm{LDHTS}}/\mathcal{C}^{\mathrm{LACO}}\right)\right] \times 100\%$, which is illustrated in Fig. 6 and indicates that LDHTS-ACO-OFDM is appreciably less complex than LACO-OFDM. Moreover, the gain increases with an increase in number of superimposed layers, approaching $\approx 43\%$ for $\{L, \log_2(N)\} = 5$. The complexity of LACO-OFDM is evaluated considering the most recent article [5]. However, an implementation with lower order IDFT/DFT is presented in [4]. It should be recognized that an implementation of LDHTS-ACO-OFDM with lower order IDHT/DHT is likewise feasible.

IV. Conclusions

In this letter, a spectrally augmented variant of DHTS-ACO-OFDM, i.e., LDHTS-ACO-OFDM is proposed. LDHTS-ACO-OFDM stack layers of DHTS-ACO-OFDM, where each superimposed layer modulates the empty subcarriers left by the preceding layer. Unlike other O-OFDM schemes, where half of the subcarriers are sacrificed to integrate HS, in LDHTS-ACO-OFDM, all the subcarriers can be modulated. Moreover,

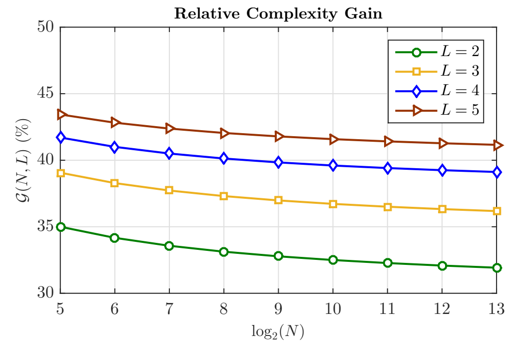

Fig. 6: Gain in complexity of LDHTS-ACO-OFDM over LACO-OFDM.

LDHTS-ACO-OFDM is less complex than LACO-OFDM, while it manifests lower PAPR and maintains 3 dB BER improvement over LACO-OFDM in a dispersive channel.

References

[1] Carruthers J. B. and J. M. Kahn. Multiple-subcarrier modulation for nondirected wireless infrared communication. *IEEE J. Sel. Areas Commun.*, 14(3):538–546, 1996.

[2] J. Armstrong and A. J. Lower. Power efficient optical OFDM. *Electron. Lett*, 42(6):370–372, 2006.

[3] S. C. J. Lee, S. Randel, F. Breyer, and A. M. J. Koonen. PAM-DMT for intensity-modulated and direct-detection optical communication systems. *IEEE Photo. Tech. Lett.*, 21(23):1749–1751, 2009.

[4] Q. Wang, C. Qian, X. Guo, Z. Wang, D. G. Cunningham, and I. H. White. Layered ACO-OFDM for intensity-modulated direct-detection optical wireless transmission. *Opt. Express*, 23(9):12382–12393, 2015.

[5] X. Zhang, R. Wang, Q.and Zhang, S. Chen, and L. Hanzo. Performance analysis of layered ACO-OFDM. *IEEE Access*, 5:18366–18381, 2017.

[6] M. S. Islim and H. Haas. Augmenting the spectral efficiency of enhanced PAM-DMT-based optical wireless communications. *Opt. Express*, 24(11):11932–11949, 2016.

[7] A. W. Azim, Y. Le Guennec, and G. Maury. Decision-directed iterative methods for PAPR reduction in optical wireless OFDM systems. *Opt. Commun.*, 389:318–330, 2017.

[8] C. Wu, H. Zhang, and W. Xu. On visible light communication using LED array with DFT-spread OFDM. *IEEE ICC*, pages 3325–3330, 2014.

[9] J. Zhou and Y. Qiao. Low-PAPR asymmetrically clipped optical OFDM for intensity-modulation/direct-detection systems. *IEEE Photon. J.*, 7(3):1–8, 2015.

[10] H. Elgala, R. Mesleh, and H. Haas. Practical considerations for indoor wireless optical system implementation using OFDM. *IEEE ConTEL*, pages 25–29, 2009.

[11] M. Wolf, S. A. Cheema, M. A. Khalighi, and S. Long. Transmission schemes for visible light communications in multipath environments. *Intl. Conf. on Transparent Opt. Networks*, pages 1–7, 2015.

[12] K. Lee, H. Park, and J. R. Barry. Indoor channel characteristics for visible light communications. *IEEE Commun. Lett.*, 15(2):217–219, 2011.

[13] D. Tsonev, S. Videv, and H. Haas. Unlocking spectral efficiency in intensity modulation and direct detection systems. *IEEE J. Selec. Areas Commun.*, 33(9):1758–1770, 2015.

[14] B. Ranjha, Z. Zhou, and M. Kavehrad. Performance analysis of precoding-based asymmetrically clipped optical orthogonal frequency division multiplexing wireless system in additive white Gaussian noise and indoor multipath channel. *Opt. Eng.*, 53(8):086102–086102, 2014.

[15] S. G. Johnson and M. Frigo. A modified split-radix FFT with fewer arithmetic operations. *IEEE Trans. Sig. Process.*, 55(1):111–119, 2007.

[16] J. Zhou, Y. Qiao, Z. Cai, and Y. Ji. An improved scheme for flip-OFDM based on Hartley transform in short-range IM/DD systems. *Opt. Express*, 22(17):20748–20756, 2014.